

Photodynamics of $(\text{Cl}_2)_n$ Clusters Trapped in Solid Krypton

G. J. Hoffman and V. A. Apkarian*[†]

Department of Chemistry, University of California, Irvine, California 92717 (Received: March 11, 1991;
In Final Form: May 6, 1991)

Emission and excitation spectra of Cl_2 clusters isolated in solid Kr, matrix and free-standing crystal, are reported. A broadened emission progression in the crystal is ascribed to dimeric $A' \rightarrow X$; additional molecular aggregates are evident in the matrix. The dimeric A' state relaxes radiatively with a lifetime identical with that of the monomer ($\tau = 49 \pm 1$ ms), whereas the B state undergoes nonradiative relaxation on a time scale that competes with predissociation. A significant difference in intermolecular binding between excited and ground states is inferred. The clusters do not undergo permanent dissociation at an excess energy of 1.5 eV.

Molecular clusters trapped in rare-gas solids provide a fascinating conceptual model for the investigation of molecular dynamics in tightly oriented systems. Many-body interactions, intermolecular potentials, energy transfer, and biomolecular reaction dynamics are possible targets of such investigations. Spectroscopic and dynamical information obtained from such studies should also be complementary to the related, well-established field of cluster dynamics in molecular beams. In the literature of matrix isolation spectroscopy, there is a wealth of information on structure and isolation properties of dimers, trimers, and larger molecular aggregates, mostly obtained by infrared studies.¹ However, investigations of dynamics and electronic spectroscopy of such systems are rather scarce. Notable exceptions are the studies on $(\text{O}_2)_2$ isolated in Ne^2 and Ar ,³ and $(\text{N}_2)_n$ trapped in Xe ,⁴ which have provided significant insights into the intermolecular energy transfer and relaxation dynamics of these clusters. In this letter we report exploratory results obtained by laser-induced fluorescence studies in Cl_2 clusters trapped in solid Kr.

Studies were conducted in both free-standing crystals and in matrices of Kr. The particular cryostat used in these experiments could reach a base temperature of only 22 K, at which temperature the samples were prepared. The crystal growth techniques have previously been discussed;⁵ pulsed deposition was used for the preparation of the matrices. Either an excimer or an excimer-pumped dye laser (Lambda Physik EMG 201 MSC/FL 3002) was used as excitation source. Fluorescence was dispersed by a 1.0-m monochromator (Spex 1702) and detected by using a cooled photomultiplier tube with a flat spectral response in the range 200–850 nm (Hamamatsu R943-02). A gated photon counter was used for the acquisition of data (Stanford Research Systems SR400).

Emission spectra obtained with 308-nm excitation, which corresponds to the first continuum absorption of Cl_2 ($^1\Pi_{1u} \leftarrow ^1\Sigma_{0g}^+$), are shown in Figure 1, traces a and b. Trace a is from a matrix at 22 K, with a concentration of 1:1000 Cl_2 :Kr; the spectrum in trace b is from a free-standing crystal at 22 K, prepared from a sample of 1:50000 Cl_2 :Kr. The long-wavelength cutoff in these spectra is due to the spectral response of the photomultiplier. Excitation at 308 nm leads to a strictly dissociative state in Cl_2 ; however, a nearly perfect cage effect ensures that the Cl atoms recombine, and it is this recombinant emission that is observed.⁶ The recombination of the caged atoms populates all states that correlate with $\text{Cl}(^2P_{3/2})$, namely, A , A' , and X . The sharp progressions in both spectra correspond to monomeric Cl_2 emission which has previously been assigned to $A'(^3\Pi_{2u}, v=0) \rightarrow X(^1\Sigma_{0g}^+, v=v')$.⁶ They occur in triplets, reflecting the natural isotopic abundance of ^{35}Cl and ^{37}Cl . The progression of much broader lines, which appear midway between the monomer peaks, is assigned to emission from $(\text{Cl}_2)_n$ aggregates. That such aggregates emit should not be surprising, as emission from solid Cl_2 showing vibronic structure in the same spectral range has been reported previously.⁷

The cluster emission peaks are broader and less symmetric in the matrix spectrum (Figure 1a) than those in the crystal spectrum (Figure 1b). However, if detection of the matrix emission is delayed, as in Figure 2b, the asymmetry is not apparent—the blue tail on individual cluster bands disappears, and the spectrum more closely resembles that of the crystal. Thus, the matrix gives evidence for at least two different aggregate species: one relatively short lived ($\tau = 13 \pm 1$ ms) and the other longer lived ($\tau = 49 \pm 1$ ms). The long-lived species emission has a lifetime virtually identical with that of the monomer emission (48 ± 1 ms). The fact that this long-lived aggregate seems to predominate in the crystal, whose Cl_2 concentration is quite low, suggests that this species is most likely the $(\text{Cl}_2)_2$ dimer. The shorter lived species present in the matrix may be either a larger aggregate, such as a trimer, or a dimer trapped in an unfavorable geometry. It is most likely that a distribution of such sites contributes to the asymmetric line shape observed when total fluorescence is recorded from the matrix. Species in unfavorable sites would not be expected in the crystal since crystal samples are prepared under conditions that guarantee annealing during growth. Given the similarity in lifetimes and similarity in the spectra, the broad progression is assigned to recombinant emission over the $A' \rightarrow X$ transition of the dimer.

The most mundane dynamical information that can be extracted from the stability of emission spectra is that, as in the case of the monomer, the clustered species do not undergo permanent dissociation in solid Kr. Neither the absolute emission intensities nor the cluster-to-monomer relative emission intensities change with time during extensive periods of irradiation at 308 nm. This observation would imply that quantum yields of dissociation for both species are similarly negligible. In the case of monomeric Cl_2 in Ar and Kr matrices, previous studies have set an upper limit for photodissociation quantum yields of 10^{-6} , at 308 nm.⁷ Excitation, at 308 nm corresponds to 1.5 eV in excess of the gas-phase dissociation limit of Cl_2 .

It is possible to assign v'' for the $(\text{Cl}_2)_2$ progression by comparing the spectral intervals with those of the monomer. If the ground-state vibrational frequency and anharmonicity in the dimeric species are assumed to be the same as those of the isolated monomer, then the assignment shown in Figure 1b results. This tentative assignment would imply that (a) the electronic origin of the emission is reduced by 750 cm^{-1} and (b) since the dimeric

(1) Ball, D. W.; Kafafi, Z. H.; Fredin, L.; Hauge, R. H.; Margrave, J. L., Eds. *A Bibliography of Matrix Isolation Spectroscopy*; Rice University Press: Houston, 1988.

(2) Goodman, J.; Brus, L. E. *J. Chem. Phys.* 1977, 67, 4398; 1977, 67, 4408.

(3) Becker, A. C.; Schurath, U.; Dubost, H.; Galaup, J. P. *Chem. Phys.* 1988, 125, 321.

(4) Kühle, H.; Bahrdt, J.; Föhling, R.; Schwentner, N.; Wilcke, H. *Phys. Rev. B* 1985, 31, 4854.

(5) See, for example: Kunttu, H.; Lawrence, W. G.; Apkarian, V. A. *J. Chem. Phys.* 1991, 94, 1693.

(6) Bondybey, V. E.; Fletcher, C. *J. Chem. Phys.* 1976, 64, 3615.

(7) Fajardo, M. E.; Withnall, R.; Feld, J.; Okada, F.; Lawrence, W.; Wiedeman, L.; Apkarian, V. A. *Laser Chem.* 1988, 9, 1.

[†] Alfred P. Sloan fellow.

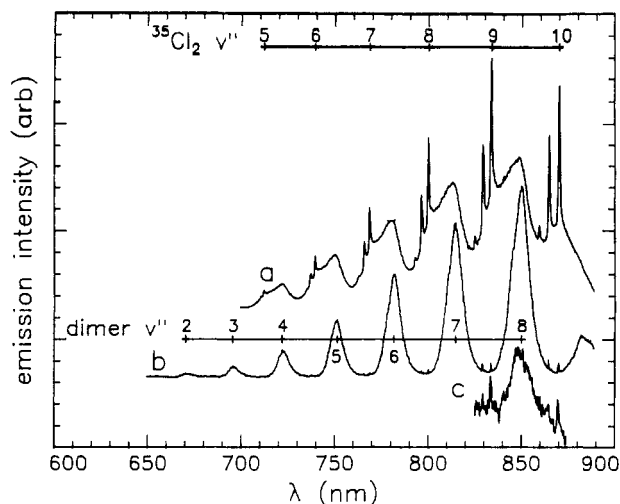


Figure 1. (a) Emission spectrum of a 1:1000 Cl_2 in Kr matrix prepared at 22 K, excited at 308 nm (monochromator slit width = 100 μm). The assignment of the $^{35}\text{Cl}_2$ monomeric transitions is from ref 6. (b) Emission spectrum of a 1:50 000 Cl_2 in Kr free-standing crystal prepared at 22 K, excited at 308 nm (monochromator slit width = 200 μm). Monomer emission lines are present as very small, sharp lines between the cluster features. (c) Same as in (b) except using 505-nm excitation (monochromator slit width = 1 mm). Note that the integrated emission intensity of the dimer line, compared to the monomer lines, has decreased by a factor of 50 from (b).

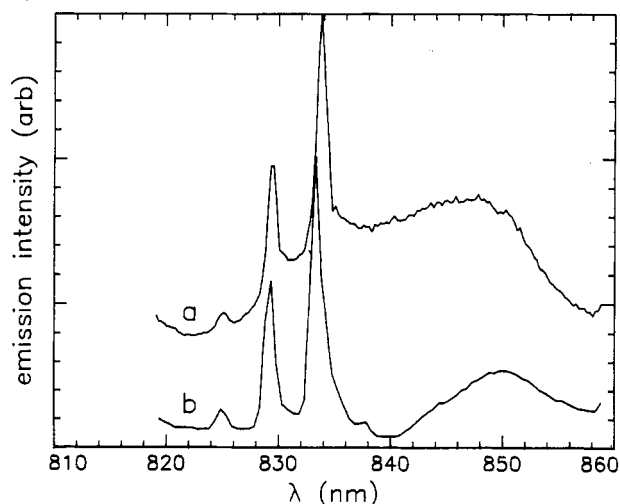


Figure 2. Emission spectra from use of gated detection from the 1:1000 Cl_2 :Kr matrix, excited at 308 nm (monochromator slit width = 400 μm). (a) Prompt spectrum: gate delay = 5 μs , gate width = 40 ms. This is essentially a section of Figure 1a shown in greater detail. (b) Delayed spectrum: gate delay = 80 ms and gate width = 100 ms. The blue tail of the cluster emission feature in (a) has collapsed in (b). The peak positions and shapes in (b) more closely resemble those in Figure 1b.

progression starts at lower v'' , the difference between internuclear separation in the A' and X states is smaller in the dimer than in the monomer. The similarity in the intensities of the emission band envelopes implies that Franck-Condon factors are similar in clustered and monomeric species, giving further credence to the spectral assignment. A more complete spectrum would clearly enable a firmer assignment.

The dimeric emissions are broadened to the extent of obscuring the expected isotopic splitting of the lines—save a slight blue shoulder that appears on all dimeric transitions (see Figure 1b). If inhomogeneous broadening due to multiple site trapping is a significant contributor to the widths of the lines, the emission spectrum should depend on excitation wavelength. We have failed to see such a dependence for excitation to the B state, leading us to the conclusion that the observed line widths are dominated by homogeneous broadening. A significant change in intermolecular potentials, and therefore dimer geometries, between excited and

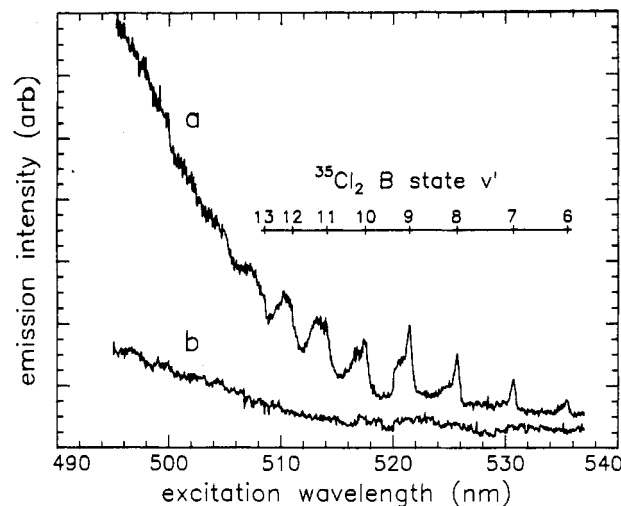


Figure 3. (a) B-state excitation spectrum of the $^{35}\text{Cl}_2$ ($A'(v'=0) \rightarrow X(v''=9)$) emission line for a 1:1000 Cl_2 in Kr matrix at 30 K. The assignment is from ref 6. (b) B-state excitation spectrum of the $(\text{Cl}_2)_2$ ($A'(v'=0) \rightarrow X(v''=8)$) emission line for the same sample. No structure is evident, and emission intensity increases more slowly toward bluer excitation wavelength than in (a).

ground states could in principle explain the origin of the line widths. The reduction of 750 cm^{-1} in electronic origin of the transition clearly implies significant stabilization of the Cl_2 -(A')- Cl_2 (X) excited dimer relative to the ground-state Cl_2 (X)- Cl_2 (X). It is therefore reasonable to expect that the vertical transition from the excited-state minimum would terminate on the repulsive wall of the intermolecular potential on the ground surface. Such an excimeric bound-to-repulsive transition along the internuclear coordinate, with negligible perturbation of the ground-state molecular potential, provides a natural explanation for both the widths and positions of the dimeric $A' \rightarrow X$ emission progression. The line widths in this case would be determined by the gradient of the intermolecular potential on the ground surface evaluated at the geometry of the excited-state potential minimum. Note, however, that there are dynamical consequences associated with such potential surfaces. A large change in intermolecular coordinates would imply that the vertical transition leads to the direct creation of local phonons, and accordingly, efficient phonon-assisted vibrational relaxation of the molecular vibrations in the ground state is to be expected. The latter consideration alone, namely, efficient relaxation of the terminal vibrational levels, provides an alternative mechanism for the observed spectrum. If indeed the observed line widths were dominated by vibrational relaxation in the ground state, then a lifetime of ~ 0.2 ps would be inferred from the spectrum. The relative contributions of these distinct mechanisms to the observed line shapes are presently being investigated by real-time measurements.

Emission due to excitation of the $B(^3\Pi_{0g+})$ state has also been investigated. Figure 1c shows the emission spectrum of the free-standing crystal upon excitation at $\lambda = 505$ nm. The most striking feature of this spectrum, when compared with Figure 1b, is the dramatic (50-fold) decrease in dimer/monomer relative intensities. This would suggest very different branching ratios for population of the A' state when the predissociative $B(^3\Pi_{0g+})$ state is accessed as opposed to the dissociative excitation at 308 nm. Excitation spectra recorded in the matrix sample while monitoring the monomeric and dimeric emissions are illustrated in Figure 3. The monomer excitation spectrum, Figure 3a, is similar to that previously reported in solid Ar.⁶ Several bound vibrations in the B manifold can be observed that show typical phonon sidebands. The lines, however, broaden and merge with a continuum at shorter wavelengths due to contributions from stronger interactions with the lattice and due to the access gained to the repulsive walls of the A manifold. Although the dimeric species is populated in the same spectral range, the excitation spectrum, Figure 3b, shows no vibronic progression within the limited dynamic range of the experiment. Presumably, the vi-

brational resonances are broadened beyond recognition in the dimeric B state due to lifetime shortening. Furthermore, to rationalize the dramatic difference in branching ratios, the lifetime shortening in the dimer cannot be entirely ascribed to predissociation but rather to efficient nonradiative relaxation from the B to the X states bypassing the A and A' manifolds.

On the basis of the observed emission lifetimes, we are led to conclude that the A' manifold in the dimeric species is essentially unperturbed. On the other hand, the absence of structure in the excitation spectrum to the B state indicates that the B state is strongly perturbed in the dimer or at least that the vertically accessed states in the B manifold undergo rapid relaxation. This observation is also consistent with the notion that there is a significant difference between the ground- and excited-state intermolecular potentials of the dimer, as previously argued on the basis of the (A' → X) emission line widths. A consideration of the molecular orbitals involved in these states gives clues as to the structure of the excited- and ground-state intermolecular potentials. The ground-state potential is due to interactions between closed-shell molecules and therefore expected to be determined by the balance between dispersive attractive forces and electron-electron repulsion between the filled orbitals. A parallel or a D_{2d} geometry would be expected to minimize the energy of such a dimer. Quadrupolar interactions, which would favor a T_m geometry, are known to be unimportant from structure analyses of Cl₂ crystals.⁸ Excitation into the ³Π manifold (B, A, and A' states) involves the promotion of a nonbonding π electron into

the antibonding σ* orbital, reducing the molecular binding by a bond order of one-half. Accordingly, reduction in electronic repulsion for side-on intermolecular binding, and therefore a tighter geometry in the excited state, is to be expected. These considerations rationalize the observed differential binding and the large change in intermolecular coordinates that was inferred from the emission and excitation line shapes. However, it is not possible to ascertain the dimer geometry at present. As a further probe of structure and dynamics, we have carried out polarization measurements in the crystalline samples. No net polarization is observed in emission. This null result does not lead to unique interpretations.

Work is presently in progress to put some of the above conclusions on a firmer footing. It should, however, be clear that a wealth of information regarding intermolecular dynamics can be extracted from such studies and that extension of such studies to clusters of unlike species should be particularly useful for probing reactive dynamics. The present results also indicate that, due to the very rapid relaxation of the vibronic states in the B manifold, it may be difficult to observe Cl₂ clusters in molecular beams if the B state is used as detection intermediate. Finally, we point out that despite the very high dilution (1:50 000), the dominant emission in the crystal is due to dimers. While this may vary as a function of conditions of crystal growth, this observation illustrates the danger in assumptions of molecular isolation based on dilution arguments alone.

Acknowledgment. This research was funded by the U.S. Air Force Astronautics Laboratory under Contract S04611-90-K-0035.

(8) Williams, D. E.; Hsu, L.-Y. *Acta Crystallogr.* 1985, A41, 296.

Two-Photon Direct Laser-Assisted Reaction between Xe and ClF

J. Qin, T. O. Nelson, and D. W. Setser*

Department of Chemistry, Kansas State University, Manhattan, Kansas 66506 (Received: March 12, 1991; In Final Form: May 16, 1991)

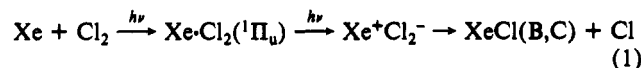
The two-photon, laser-assisted reaction between Xe and ClF under dilute gas conditions is demonstrated. The only product is XeCl(B,C) in contradistinction to the reactions of Xe(6s) and Xe(6p) atoms with ClF or the reaction of ClF(4s^{1,3}Π) with Xe, which give both XeCl(B,C) and XeF(B,C). The excitation spectra from the laser-assisted reaction of Xe/ClF and Xe/Cl₂ are compared. Arguments based upon product-state distributions and the laser intensity dependence are summarized to favor a direct, rather than a stepwise, mechanism for the laser-assisted reactions of Xe with halogens under dilute gas conditions.

I. Introduction

There has been considerable interest in the one-color, two-photon, laser-assisted reaction (LAR) of rare-gas atoms with halogen molecules as a direct probe of the reactive ionic potential with respect to the ground-state van der Waals potential. Experiments have been done with Xe/Cl₂, Xe/ICl, Xe/CCl₄,¹ Xe/F₂,² and Kr/F₂³ in dilute gases, as well as with Xe-Cl₂ van der Waals complexes generated in a free jet expansion.⁴ LAR of Xe/Cl₂ also has been employed to generate XeCl(B,C) for subsequent kinetic studies of XeCl* and Xe₂Cl*.⁵ The two-photon

LAR in liquid or solid mixtures of rare gases and halogen also has drawn attention,⁶ and there is some correspondence with gas-phase processes. We will report the excitation spectrum for the two-photon LAR of Xe/ClF and demonstrate that product specificity can be achieved. This opens a new dimension for study of stereochemical constraints to entrance channels in bimolecular reactions.⁷

A detailed model for the excitation mechanism of the one-color, two-photon LAR reaction of Xe with halogen molecules (X₂) remains to be developed. Ku and Setser¹ proposed a direct mechanism based on low-pressure experiments with Xe/Cl₂:



A second-order dependence for generation of vibrationally excited XeCl(B,C) molecules was observed for a wide range of laser

(1) (a) Ku, J. K.; Inoue, G.; Setser, D. W. *J. Phys. Chem.* 1983, 87, 2989. (b) Ku, J. K.; Setser, D. W. In *Photochemistry and Photophysics above 6 eV*; Lahmani, F., Ed.; Elsevier: Amsterdam, 1985.

(2) Nelson, T. O. Ph.D. Thesis, Kansas State University, 1991.

(3) Nelson, T. O.; Setser, D. W. *Chem. Phys. Lett.* 1990, 170, 430.

(4) (a) Jouvét, J. C.; Boivineau, M.; Duval, M. C.; Soep, B. *J. Phys. Chem.* 1987, 91, 5416. (b) Boivineau, M.; LeCalve, J.; Castex, M. C.; Jouvét, C. *Chem. Phys. Lett.* 1986, 128, 528; 1986, 130, 208. (c) These authors studied the two-photon excitation of bound Xe-Cl₂ van der Waals molecules. The reaction dynamics apparently differ from our dilute gas experiments because low vibrational energy XeCl(B,C) molecules were generated starting from the bound Xe-Cl₂ van der Waals molecules.

(5) Quinones, E.; Yu, Y. C.; Setser, D. W.; Lo, G. *J. Chem. Phys.* 1990, 93, 333.

(6) (a) Fajardo, M. E.; Withnall, R.; Feld, J.; Okada, F.; Lawrence, F.; Wiedeman, L.; Apkarian, A. P. *Laser Chem.* 1988, 9, 1. (b) Okada, F.; Wiedeman, L.; Apkarian, V. A. *J. Phys. Chem.* 1989, 93, 1267.

(7) (a) Levine, R. D. *J. Phys. Chem.* 1990, 94, 8872. (b) Buelow, S.; Noble, M.; Radhakrishnan, G.; Reisler, H.; Witting, C.; Hancock, G. *J. Phys. Chem.* 1986, 90, 1015.